

Document downloaded from:

<http://hdl.handle.net/10251/202040>

This paper must be cited as:

Alonso-Pandavenes, O.; Torres, G.; Torrijo, F.; Garzón-Roca, Julio (2022). Basement tectonic structure and sediment thickness of a valley defined using HVSr geophysical investigation, Azuela valley, Ecuador. Bulletin of Engineering Geology and the Environment. 81(5):1-14. <https://doi.org/10.1007/s10064-022-02679-y>



The final publication is available at

<https://doi.org/10.1007/s10064-022-02679-y>

Copyright Springer-Verlag

Additional Information

Journal: Bulletin of Engineering Geology and the Environment
Manuscript Number: BOEG-D-20-00595
Title: Basement tectonic structure and sediment thickness of a valley defined using HVSR geophysical investigation. Azuela valley. Ecuador.
Authors: Olegario Alonso-Pandavenes, Gabriela Torres, Francisco Javier Torrijo and Julio Garzón-Roca
Status: Revised version

Response to the reviewers and description of the changes made up in the first revised version of the manuscript

Initial Considerations

First of all, the authors would like to thank the contribution of the reviewers for their thorough examination of the manuscript and valuable comments, which will undoubtedly enhance the manuscript's quality. The authors have tried to attend the comments and suggestions of the Reviewers in this revised version of the manuscript. All the comments made by the reviewers are addressed individually. In each case, the reviewer's comment/question is presented first (in italic), then the authors' reply/answer is given next, and, finally, the action prompted by the reply is described.

In the present version of the manuscript, figures, and tables, the content was modified as recommended from Proof-Reading-Service Ltd whom have made English usage.

Editor in chief

Comment 1 – *“The citations in the text and the reference list do not follow the BOEG style. The authors should take a look at "Instructions for Authors" of BOEG and read the sections of 'Citation' and 'Reference list' under 'References' carefully. By strictly following this, the authors should make the necessary changes”*

Reply/Action – The authors thank the reviewer for their time and help. All citations (references and inside the text) were revised and completed, including the DOI where proceed.

Comment 2 – *“The English usage in the manuscript must be improved. The grammatical errors should be aptly rectified. Before submitting the revised manuscript, the authors may take help from one of the companies which provides an English editing service for scientists (for example, Edanz (www.edanzediting.com)), and include the certificate/invoice/receipt as the proof in the revised version of the manuscript”*

Reply/Action – The authors thank the reviewer for their time and valuable help. The English usage was improved and a certification of revised version of manuscript is enclosed (Proof-Reading-Service Ltd).

Reviewer #1

General comment – “This paper is well written and a classical HVSR application for seismic site effect and hazard analysis. On the other hand, there are important references missing which are directly connected with the subject and also pioneers of the related works. Therefore, it is very important for the readers for their better understating of the study with the basic studies on the subject. Authors must not only give the references of the following studies but also mention about the differences and the similarities with these studies and the current work.

1. Kanli, A.I., 2010, "Integrated Approach for Surface Wave Analysis from Near-Surface to Bedrock", Chapter 29, p. 461-476, *Advances in Near-Surface Seismology and Ground-Penetrating Radar, Geophysical Developments Series No. 15, SEG Reference Publications, Society of Exploration Geophysics Reference Publications Program, Tulsa, Oklahoma-USA. Publisher: Society of Exploration Geophysicists, American Geophysical Union and Environmental and Engineering Geophysical Society (Ed. Com.: R.D. Miller, J.D. Bradford and K. Holliger), ISBN 978-0-931830-41-9 (Series); ISBN 978-1-56080-224-2 (Volume).*

2. Kanli, A.I., Kang T.S., Pinar, A., Tildy, P., Pronay, Z., 2008, *A Systematic Geophysical Approach for Site Response of the Dinar Region, South Western Turkey, Journal of Earthquake Engineering, vol. 12:1, S2, p. 165-174.*

3. Kanli, A.I., Tildy, P., Pronay, Z., Pinar, A., Hermann, L., 2006, *VS30 Mapping and Soil Classification for Seismic Site Effect Evaluation in Dinar Region, SW Turkey, Geophysical Journal International, Volume 165, 1, p. 223-235*”

Reply/Action – The authors thank the reviewer for their time and valuable help. The three works mentioned were included as a reference and indicated that they are a new possibility of further lines of investigation from this work.

General comment – *“The paper presents an interesting study related to the basement tectonic structure and sediment thickness of a valley, based on a geophysical approach by HVSR test.*

The paper shows a good work quality both in terms of exposition clarity and presentation of results, and in terms of easy understanding of the proposed figures and tables, so, no substantial revisions are needed. Some minor editorial modify are needed”

Reply/Action – The authors thank the reviewer for their time and valuable help.

Comment 1 – *“please improve the quality text of the legend in the Fig. 2 (better if the text is in vector mode, instead of raster mode)”*

Reply/Action – The authors thank the reviewer for their time and help. The legend was corrected improving the quality of text and resized it to get better resolution for smaller sizes in Fig. 2

Comment 2 – *“please improve all the text of the Fig.3 and Fig. 9; in particular the elevation is not readable, the same for the bar-scale and for the "San Marcos dam" and "Azuela river" texts”*

Reply/Action – The authors thank the reviewer for their time and help. All text were improved with a resize and better resolution for Figures 3 and 9, including a new bar-scale and elevation numbers. Also orthographic error corrected.

Comment 3 – *“please improve the quality text of the legend in the Fig. 4 (better if the text is in vector mode, instead of raster mode)”*

Reply/Action – The authors thank the reviewer for their time and help. The legend was corrected improving the quality of text and resized it to get better resolution for Fig. 4

Comment 4 – *“Please resize the Fig.6 graphs and the legend per each: four graphs in each row is not good. Please consider maximum 2 graphs per row”*

Reply/Action – The authors thank the reviewer for their time and help. The graphs on Fig. 6 were rescaled and using 2 graphs per row. The axis legend and units are now clearer than initial figure. Also corrected an orthographic error in text of figure

Comment 5 – *“Please improve the fig.7 and 8 axis legend: is with poor resolution”*

Reply/Action – The authors thank the reviewer for their time and help. The size and resolution in both axes were improved for figures 7 and 8

Comment 6 – *“Please insert a figure (best if a photo) of the in-situ carried out HVSR test”*

Reply/Action – The authors thank the reviewer for their time and help. A picture of equipment in area of investigation was included inside the Fig. 5 (field data example) with the purpose of don't make changes in total number of figures.

Comment 7 – “About the importance of the in-situ test authors may evaluate to cite this work:

- Ferraro A., Grasso S., Massimino M. R., Maugeri M. (2015) - Influence of geotechnical parameters and numerical modelling on local seismic response analysis.

- Castelli, F., Cavallaro, A., Ferraro, A., Grasso, S., Lentini, V., Massimino, M.R. (2018) - Influence of geotechnical parameters and numerical modelling on local seismic response analysis.”

Reply/Action – The authors thank the reviewer for their time and help. Included in bibliography first work (from 2015) and comments inside text about it. Second one *Castelli, F., Cavallaro, A., Ferraro, A., Grasso, S., Lentini, V., Massimino, M.R. (2018) - Influence of geotechnical parameters and numerical modelling on local seismic response analysis.*” can't be found

Yours sincerely,

Mr. Olegario Alonso-Pandavenes (the corresponding author)
(omalonso@uce.edu.ec)

[Click here to view linked References](#)

1 **BASEMENT TECTONIC STRUCTURE AND SEDIMENT THICKNESS OF A VALLEY**
2 **DEFINED USING HVSR GEOPHYSICAL INVESTIGATION. AZUELA VALLEY.**
3 **ECUADOR**

4 Olegario Alonso-Pandavenes^a, Gabriela Torres^b, Francisco Javier Torrijo^{c,d} and Julio Garzón-Roca^e

5
6 ^a Geology and Mining Engineering Faculty, FIGEMPA, Universidad Central del Ecuador, Quito, 170129. E-mail address: omalonso@uce.edu.ec

7
8 ^b Geology and Mining Engineering Faculty, FIGEMPA, Universidad Central del Ecuador, Quito, 170129. E-mail address: gftorres@uce.edu.ec

9
10 ^c Department of Geotechnical Engineering, Universitat Politècnica de València, Camino de Vera s/n, 46022, Valencia, Spain. E-mail address: fratorec@trr.upv.es

11
12 ^d Research Centre PEGASO, Universitat Politècnica de València, Camino de Vera s/n, 46022, Valencia, Spain. E-mail address: fratorec@trr.upv.es

13
14 ^e Department of Geodynamics (GEODESPAL), Faculty of Geology, Complutense University of Madrid, 28040, Madrid, Spain. E-mail address: julgarzo@ucm.es

15
16 *Corresponding author. Tel.: +593 995608066. omalonso@uce.edu.ec

17
18 **Abstract**

19 The use of a small set of boreholes, as fixed information of the basement, combined with the analysis
20
21 of microtremor surveys can provide a transversal detailed section of a valley. In this paper, the
22
23 horizontal to vertical spectral ratio (HVSR) technique was applied as a quick and economic method
24
25 to establish the thickness of the sediments existing over the rock basement in the San Marcos dam
26
27 area, located at the Azuela valley (Cayambe, Ecuador). Previous investigations conducted for the
28
29 construction of the dam, with a length of 700 m, did not reach the bottom of the valley; only the
30
31 abutments were properly defined, where the rock being close to the ground surface at those areas.
32
33 Involving a few boreholes as control points, a relation between the natural frequency of the ground
34
35 vibration and the sediment thickness was established. 20 HVSR single station points were measured
36
37 and analyzed in the three main directions (N-S, E-W and Z) of the components of the ground natural

29 vibration (rumour) and using the natural vibration frequency at each point, a correlation was
130 established with the sediment thickness. From that point, the geological cross-section of the bottom
2
31 of the valley could be delineated, revealing some tectonic structures (faults) not defined in the
4
5
632 previous geotechnical investigations and whose evidence may be useful in further control dam
7
833 settlement studies. The proposed formulation can also be used as a quick tool to accurately investigate
9
10
1134 the area around the dam and define other tectonic structures not previously evidenced.

12
13
1435
15
16
1736 **Keywords:** HVSR; Microtremor; H/V Spectral ratio; Depth of bedrock; Azuela valley

18
19
2037
21
2238 **1. Introduction**

23
24
2539 Seismic vibrations that result from either anthropic or natural sources are called microtremors. They
26
27
2840 can vary in energy daily or weekly, or in the position of sources, but they are still constant in
29
3041 frequency over time (Asten 2004; Bonnefoy-Claudet et al. 2004; SESAME 2004). Nakamura (1989)
31
32
3342 hypothesised that the vertical component of ambient noise has the characteristics of source to
34
3543 sediments surface ground and is relatively influenced by Rayleigh waves on the sediments. Therefore,
36
37
3844 the vertical component may be used to remove both the source and the Rayleigh wave effects from
39
4045 the horizontal components. This technique is called HVSR (Horizontal to Vertical Spectral Ratio),
41
4246 H/V, or the Nakamura technique, and it can be applied both in earthquake research (determination of
43
44
4547 fundamental periods of vibration) and in geological logging (classification of geological materials
46
4748 using V_s and V_{s30}) through the analysis of an ellipticity curve (Nakamura 1989; Delgado et al. 2015;
48
49
5049 Pamuk et al. 2019; Jirasakjamroonsri et al. 2019). The HVSR technique can identify the fundamental
51
5250 resonant frequency of a sedimentary layer and its implied amplification factors. This has been shown
53
54
5551 by other researchers (Ohmachi et al. 1991; Lermo et al. 1992; Field and Jacob 1995; Kanli 2010) who
56
5752 used the H/V ratio of noise to identify the fundamental resonant frequency of sediments. The
58
5953 application of this technique only requires a high geophysical impedance (relationship between the
60
61
62
63
64
65

54 bulk density of a medium and the velocity of the seismic wave propagating through it) contrast of
155 more than two times between existing media to obtain successful results (Nakamura 1998; Vella et
2
3
4
5
6
7
8
9
10
11
12
13
14
15
16
17
18
19
20
21
22
23
24
25
26
27
28
29
30
31
32
33
34
35
36
37
38
39
40
41
42
43
44
45
46
47
48
49
50
51
52
53
54
55
56
57
58
59
60
61
62
63
64
65

Since 2006, the Autonomous Decentralized Government of the Province of Pichincha (Ecuador), hereafter GADPP, has been building an irrigation system. This system involves the construction of a fine-grained core earth dam to the south of the San Marcos lagoon, in the Azuela River valley, which serves as a reservoir for water distribution (www.pichincha.org.ec). The reservoir is expected to start to being filled by the end of 2020, and the commissioner needs to control the responses of the dam's foundation and the ground until reaching the final capacity (13 m above the base level of the lagoon). Knowledge about the geology and the structure of the bottom of the valley and the sediments' thicknesses are both required for this process, but they are undetermined for now: the tests (boreholes) and surveys (seismic refraction) conducted in the geological and geotechnical study (in 2009) did not reach the level of the bedrock, especially in the central zone of the infrastructure where a greater thickness of sediments exist (GADPP 2009).

Thus, this paper shows the application of the HVSR technique to quantify the thickness of the sedimentary materials overlying the basement of the San Marcos dam. The high contrast of impedances that exists among the recent sediments (flow of pyroclasts, volcano sedimentary materials, and alluvial and lacustrine sediments) and the compact basement formed by lavas belonging to the Angochagua formation in the study area enabled the application of the HVSR technique. Both bulk density and seismic velocity have a high difference in values that gives the needed impedance contrast: previous studies (GADPP 2009) have shown that the velocity of the primary waves (V_p) was around 2000 m/s in the highly compacted sediments and over 4000 m/s in the basement rock (lavas); this results in a ratio of 2 between them (also in impedance).

The identification of the position of the basement (bedrock) of the San Marcos dam was obtained from the results of a Rayleigh wave analysis and the ratio of the H/V components, by using a mathematical formulation that relates the fundamental frequency of vibration of the ground and the

80 thickness of the sediments (Chang et al. 2015). This completely determined the east-west cross-
81 section of the basement, and the structure of the Azuela River was clearly defined. The established
2 relation may provide a quick and economical tool for prospecting bigger areas around the dam to
3
4
5
6
7
8
9
10
11
12
13
14
15
16
17
18
19
20
21
22
23
24
25
26
27
28
29
30
31
32
33
34
35
36
37
38
39
40
41
42
43
44
45
46
47
48
49
50
51
52
53
54
55
56
57
58
59
60
61
62
63
64
65

85 2. Geographical setting and geological framework

86 The valley of Azuela River is located in the municipality of Cayambe, in the eastern part of the
87 province of Pichincha, in the north of Ecuador (**Fig. 1**). It was originally a valley embedded in a deep
88 V shape enhanced by the existence of north-south and northwest-southeast direction faults, which
89 have been covered by sediments from the Holocene to actual times (Torres 2018). The studied area
90 is geomorphologically characterised by the presence of a lagoon, San Marcos, which was formed
91 after a past eruption of the Cayambe volcano. This natural water reservoir is located to the north,
92 about 10 kilometres north of the crater (**Fig. 2**), in which a pyroclastic flow blocked the valley and
93 generated water and sediment retention (Samaniego et al. 1998).

94 The geology of the area is characterised by the presence of a Pleistocene basement formed by lavas
95 and compact volcanic products (cemented pyroclasts) belonging to the Angochagua formation. A
96 sequence of volcanic materials (flows, pyroclastic, and ash) and glacial, alluvial, and lacustrine
97 sediments have been deposited over them (Torres 2018).

98 The geological cartography (**Fig. 2**) was performed by GADPP (2009) and subsequently reviewed by
99 Torres (2018). It shows how the pyroclastic flowed from the Cayambe volcano (to the southwest,
100 outside the image) blocked the valley of the Azuela River. These materials have been dated to 4000
101 B.P., and came from a San Marcos type eruption, one of the strongest scenarios that could produce
102 this volcano. These pyroclastic sediments functioned as a natural dam that allowed the formation of
103 the San Marcos lagoon and the sedimentary series on which the constructed dam is currently located
104 (Samaniego et al. 2004).

105 The geomorphology of the valley area presents an accentuated V shape which has been gently
106 softened by glaciers (the Ismuquiru river valley, just to the west of the Azuela valley, has a clear U-
107 shape typical of glacial events) with slopes at its flanks of 16° in the west and 20° in the east. The
108 eastern flank, over the dam crest, has flatter slopes and a plain area raised 100 m over the lagoon
109 water level. This could be due to the effects of glacial erosion. The slopes to the west keep the original
110 acute form of the valley, probably because they were formed by the action of the north-south direction
111 fault that would run through the centre of the current lagoon (Torres 2018). The actual level of the
112 land in this area is at an average of 3420 m above sea level.

113 The structural features of the area, like faults and folds, are not clearly defined. Most of them are
114 covered by the sediments, overburden, and alteration soils that hide the rock and faults. These features
115 are briefly delineated in **Fig. 2**. Faults that are drawn to the west of the lagoon, with an almost east-
116 west direction, could be observed in the field. The faults that cross from north to south and northwest
117 to southeast at the centre of the Azuela valley are supported by geological sections of the dam made
118 for its construction (Torres 2018).

119 The direction of these faults is consistent with the strain processes from the subduction zone at the
120 west coast of Ecuador. The Nazca plate is subducting South American plate and this is the first origin
121 of this dextral faulting, parallel to the coast, which is also the focus of seismicity and earthquakes.
122 Thus, the San Marcos dam area is located in a high seismic hazard zone as indicated by the Ecuadorian
123 Seismic Classification (Egüez and Aspden 1993). The value of PGA calculated for rocks in this zone
124 is between 300 and 310 gal (1 gal equal to 0,01 m/s²), but it could reach between 400 and 500 gal if
125 local effects (amplification factors due to thick sedimentary cover) are considered (Torres 2018).

126 **3. Construction project and previous surveys**

127 The geological and geotechnical study for the construction of the San Marcos dam included boreholes
128 and geophysical researches conducted at the dam axis. The aim was to complement the data obtained
129 previously by GADPP (2009). **Fig. 3** shows the construction cross section of the dam along with the

130 five boreholes conducted. Perforations at or near the ends of the profile (P-7A, P-10A, PSM-3, and
131 P-9) cut the basement, while the one executed in the central zone (P8) did not reach it.

2
3
132 The geological profile showed that the basement of the valley at its central part is deeper than 75 m
4
5
6
133 (reached depth in P8 borehole), with the presence of several vertical faults accentuating this
7
8
134 deepening towards the centre and east (right edge, where the Azuela River is located). Measured
9
10
11
135 seismic velocities (V_p) enable the interface between the recent sedimentary materials ($V_p \approx 1725$ m/s)
12
13
136 and the pyroclastic flows ($V_p \approx 2210$ m/s) to be located at depths of 34 m from the current topographic
14
15
16
137 surface. Thus, the stratigraphic sequence in the construction zone of the dam has more than 35 m (in
17
18
138 the central zone it exceeds 40 m) of alluvial and/or lacustrine sediments (distal or low intensity of
19
20
21
139 flow) which lay over volcanic sedimentary material of pyroclastic flow type. Auxiliary 22-m-depth
22
23
240 SPT surveys done before constructing the dam foundation, demonstrated an increase of compaction
24
25
26
141 values of the ground (GADPP 2009).
27
28

29 30 31 32 33 34 35 36 37 38 39 40 41 42 43 44 45 46 47 48 49 50 51 52 53 54 55 56 57 58 59 60 61 62 63 64 65

143 An experimental study was performed at the toe of the San Marcos dam, on the downwards side of
144 the water flow and over it, using the single station HVSR technique. Since the area was saturated, the
145 station points could not be placed continuous and equal spaced as desired. A total of 17 single station
146 points were investigated close to the dam toe and spaced over, selecting harder and unsaturated soils
147 (unequal distributed in distance). Additionally, three station points were located over the crest of the
148 dam. **Fig. 3** and **Fig. 4** show the location of the station points in section and plan view, respectively.
149 Some points were not along investigated cross-section (marked as purple line in **Fig. 4**). Points 18,
150 19, and 20 were measured on the top of the dam and points 1, 4, 7, 10, 12, 17, and 14 were also
151 extrapolated to the interpreted section. Some station points were taken at the same location where
152 boreholes were performed or close to them (the exact coordinates of the position of old boreholes
153 were not available) to allow the interpretation of the results. The frequency and period of each 20
154 points measured are listed in **Table 1**.

155 The HVSR technique is based on the spectral analysis of the rumour collected on the surface of the
156 ground. The application of microtremor devices can be made through an array or alignment of
2
3
157 4 geophones, such as the ReMi technique or, as in this case, with the implantation of a single station
5
658 6 triaxial set of geophones that collect vibrations in three spatial directions (N-S, E-W, and vertically).
7
859 8 At each station point, the measuring device was implanted on the ground, as firmly as possible and
9
10
160 10 protected from the wind or external movements, with an orientation to the magnetic north of one of
11
12
161 12 the horizontal components, established with the support of a compass. The device was connected to
13
14
162 14 a computer to control the equipment and record the data. Since measurements of records need
15
16
163 16 sufficient time to obtain enough data information for further analysis, registration times of more than
17
18
164 18 20 minutes were performed, following the guidelines indicated for this type of measurements
19
20
21
22
265 22 (SESAME 2004). An example of this measured data is shown in **Fig. 5-A**, and so the used equipment
23
24
25
266 25 **(Fig. 5-C)**.
26
27
267 27 Raw data processing was carried out using the software GEOPSY v.2019 (SESAME 2004), and
28
29
30
3168 30 consisted of the generation of a windowing from 20 to 25 seconds without overlapping (**Fig. 5-B**).
31
32
369 32 To obtain the final windows to be analysed, anti-triggering filters were applied to the raw signal and,
33
34
35
3670 34 in certain cases, also to the filtered signal (low pass filter with a value of 5 Hz), cleaning the record
35
36
37
3671 36 data from transients. Transients were defined as a comparison between the average signal amplitude
37
38
39
40
4172 38 over a short time period of one second t_{STA} , STA, and the average signal amplitude over a longer time
40
41
42
4673 41 period of 30 seconds t_{LTA} , LTA. Windows that meet with STA/LTA ratios between 0.05 and 0.5 may
42
43
44
45
4674 43 be considered as stationary noise. In these spaces of the filtering window, the Fast Fourier Transform
44
45
46
47
4675 45 (FFT) was applied to each delimited space or window (Bard 2004).
46
47
48
49
50
5176 48 The curves of the horizontal components were combined squared average to obtain the relationship
49
50
51
52
5677 51 against the vertical one (H/V), previously applying a Kono and Ohmachi (1998) smoothing filter type
52
53
54
55
5678 53 of 30-40%, with cosine or triangular type windows to every component (H and V). The final HVSR
54
55
56
57
5679 55 was obtained by averaging the H/V amplitudes from all selected windows (see selected examples of
56
57
58
59
60
6180 57 this in **Fig 6**), drawing in colours calculations for every window. The average of them, as a black
58
59
60
61
62
63
64
65

181 continuous curve, and the standard deviations values for each frequency were estimated from the H/V
182 amplitude logarithm (dotted black lines in **Fig. 6**). The use of calculation parameters was selected
2
3
4
5
6
7
8
9
10
11
12
13
14
15
16
17
18
19
20
21
22
23
24
25
26
27
28
29
30
31
32
33
34
35
36
37
38
39
40
41
42
43
44
45
46
47
48
49
50
51
52
53
54
55
56
57
58
59
60
61
62
63
64
65

183 following the recommendations of the SESAME Project (Bard 2004; SESAME 2004).

184 **5. Interpretation of the field data**

185 Interpretation of the field data was done using the GEOPSY software. The relationship between the
186 dominant peak frequency (frequency of the fundamental mode of ground vibration) and the thickness
187 of sediments over the basement was quantitatively established. Nakamura (1989) and Albarello et al.
188 (2011) proposed the basis of this process considering that the Rayleigh waves, in fundamental mode,
189 dominate the environmental vibrations and these propagate in the sediments and soils that overlie a
190 basement in a homogeneous way.

191 Previous studies have shown that a large-amplitude HVSR peak can be associated to a high
192 impedance contrast between the sedimentary cover and the basement, while a low amplitude peak
193 relates to a lower contrast, indicating the presence of stiff soils (Bonneyoy-Claudet et al. 2006). In
194 1989, Nakamura suggested that the origin of the fundamental frequencies is related to the resonance
195 of the shear wave in a single layer of sediment and, therefore, the thickness of the layer (H) can be
196 related to the fundamental frequency (peak) of the H/V spectral relationship, f_o , according to the
197 relationship:

$$198 \quad f_o = \frac{n V_s}{4 H} \quad (1)$$

199 Where n are the modes of vibration without attenuation or irregularities and V_s is the velocity of the
200 shear wave in the sediments. However, the definition of this shear wave velocity in the first few
201 metres is difficult to obtain. Budny (1984), based on correlations with geotechnical surveys, indicated
202 that velocity V_s might be described as a function of depth (z) as:

$$203 \quad V_s(z) \approx V_0 (1 + z)^x \quad (2)$$

204 Where V_0 is the average shear wave velocity and x is a constant (empirically obtained). Based on
205 Budny's investigations, and using data from well logs (down-hole), Ibs von Seth and Wohlenberg

206 (1999) determined a good correlation for the peak frequencies of the H/V ratios over a wide range of
207 thicknesses (from tens to thousands of metres), following the expression:

$$Z = a f_0^b \quad (3)$$

209 Where Z is the thickness of sediments over the basement and a and b are parameters related to the
10 ground. The obtained values of those two parameters over Tertiary and Quaternary sediments in
11 Aachen (western part of the Lower Rhin riverbank) are referred to in **Table 2**. Subsequently, Parolai
12 et al. (2002), Hinzen et al. (2004), Birgören et al. (2009), and Khan and Khan (2016) made
13 adjustments in Eq. (3) according to different places tested, also obtaining different values for a and b
14 (**Table 2**). This means that in each ground (sedimentary basin) these parameters must be obtained
15 according to the conditions of the materials and their stratigraphic sequence. However, the values of
16 Ibs von Seth and Wohlenberg (1999) and Parolai et al. (2002) are generally used as a reference in
17 some publications (i.e., Khan and Khan 2016).

31 **Table 3** shows the four boreholes available at the axis of the investigated dam where bedrock was
32 reached, and the corresponding results obtained at that location using the HVSR technique. From
33 these results, parameters a and b were obtained by adjusting Eq. (3) as seen in **Fig. 7**, yielding the
34 following expression:

$$Z = 58.746 f_0^{-0.247} \quad (4)$$

45 Adjustment achieved a good match, with a coefficient of determination R^2 of 0.98 (**Fig. 7**), although
46 the contrast points used in the definition of the adjusted curve were relatively few when compared
47 with those presented by other authors (four points here versus more than 30 in the study by Ibs von
48 Seth and Wohlenberg (1999), for example).

55 **6. Analysis and discussion**

58 The fundamental frequency of ground vibrations was found to be in the range of 0.12 Hz and 61.26
59 Hz (see **Table 1**). These limits are quite broad and generate a range of dispersion which is sufficiently

230 varied to obtain good results in the analysis of the sedimentary basin because it has important
231 variations in depth throughout the investigated section.

232 The curves obtained have clear peaks in the positions 1, 5, 6, 9, and 10, without the appearance of
233 other dominant modes or peaks, being in the other position's broad peaks, but clearly denote the
234 fundamental frequency in each case. At point 12 (area away from the dam) the test showed a complex
235 curve with several peaks at high frequencies, which would indicate high impedance contrasts in
236 shallow surfaces. Regarding the viability of the H/V curves obtained in the test points 1, 4, and 7,
237 located relatively close to one another, they do not have an amplification value (A_o) in the H/V ratio
238 greater than two. So, this value exceeded those of the rest of the tests carried out (validation conditions
239 according to SESAME 2004). However, these three points were considered in the interpretation.

240 A comparison using the Eq. (3) for the different values of a and b given in **Table 2** was conducted. It
241 is interesting to note that coefficients were quite different from those obtained in studies made by
242 Parolai et al. (2002), Hinzen et al. (2004), Birgören et al. (2009), and Khan and Khan (2016). The
243 values obtained for the thickness of the sediments is presented in **Table 4**. Results can also be seen
244 graphically in **Fig. 8** (bi-logarithmic representation) where it may be observed that most of the fitting
245 lines are more tilted than the one reached in this study. This inclination is controlled by the exponent
246 of the formula, which in this case is between four and six times lower than the other proposed ones.
247 The observed numerical differences may be assigned to the nature of the materials: in all
248 investigations related to **Table 2**, the materials were composed of quartz grains and had a
249 homogeneous vertical distribution; in the present work, sediments came from an alteration of andesite
250 rocks with pyroclastic flows overlying the basement, i.e., which were all quartz poor. However,
251 further investigations are needed to confirm these differences.

252 **Fig. 9** shows the San Marcos dam profile with the position of the bedrock drawn from the
253 interpretation of the data given by the old boreholes along with the bedrock prediction interface
254 obtained by applying Eq. (4) on the points surveyed in this study. The observations reveal that the
255 bedrock interface of both interpretations is very similar for points 2, 6, 17, and 19, surveyed points

256 located used for calibrating Eq. (4) with a 4.1% of error between real depth (boreholes), and measured
257 ones (HVSr points). For the rest of the points, the results are consistent with the original drawing of
258 the basin, obtained by drilling and establishing a depth of 99.2 metres in its deepest part (supposedly
259 obtained by point 9). It should be mentioned that the values of points 1, 4, 7, 10, 14, and 17 were
260 extrapolated to the cross-section, as well as those of point 12, 175 m away from it. Nevertheless, the
261 value obtained for this one is consistent with the V-shape of the investigated valley and the closest-
262 lying ones. Although having obtained good results using Eq. (4), further research between various
263 points would be necessary to clearly define the interface of the basement in whole section.

264 **Table 4** and **Fig. 9** show the depth of the basement predicted based on the peak frequency (f_0),
265 obtained on each surveyed point using the new formulation and the ones proposed other authors. The
266 irrationality of the results is clear for the relationships of Ibs von Seth and Wohlenberg (1999), Parolai
267 et al. (2002), and Hinzen et al. (2004), where values of sediment thicknesses of more than 1000 and
268 2000 m, and less than 1 m appeared. Moreover, comparing the parameters a and b of the new equation
269 with those obtained by other authors (see **Table 2**), only those obtained by Khan and Khan (2016),
270 were close to the values established in this study. However, the results of thicknesses calculated with
271 these factors greatly differ from those obtained in the adjustment made in this investigation, having
272 only the values between 0.9 and 3.4 Hz as opposed to those that had closer values (the intersection is
273 represented in **Fig. 8**). As the values of f_0 move away from this dimension, the results differ
274 exponentially.

275 Structural information of bedrock can be extracted from **Fig. 9**. The fault name number two, at the
276 left margin of the valley (east), has been recognised in previous studies and marked at the same place
277 as has been identified in this investigation (see **Fig. 3** and **Fig. 9**). Both have a vertical scarp, dipping
278 gently toward the western side, but the difference between the two interpretations is the displacement,
279 which is currently more than ten metres against the five metres in old documents. The old
280 displacement was defined from data at borehole P-9 and helped infer this feature. In this study, data
281 measured around this place can delineate better this displacement and evaluate it more precisely.

282 On the other hand, two new fault structures have been recognised in the centre of the valley, which
283 are responsible for the depth of it: faults 3 and 4. The former is located towards the eastern side of
284 valley (at the first third). The latter is close to the centre of it (300 m from the eastern side of valley)
285 just where an inferred fault was drawn on construction section (see **Fig. 3** and **Fig. 9**). The drawing
286 of the bottom in all areas of the section had an inversed sawtooth appearance, so it was impossible to
287 define clearly a tectonic feature as faults at the western side (it could be that one was defined between
288 14 and 15 HVSR points, but not clearly). Across the publications of Alvarado (2012), the sismogenic
289 zone defined at this area is in general a strike-slip type of failure, but the oldest faults have an inversed
290 movement caused by the tension from the subduction zone. In addition, the repetition of outcrops on
291 both sides of the lagoon of lavas from the Angochagua formation leads to thinking about a system of
292 reverse faults that double the size on surface of these materials. No more detailed information can be
293 obtained about the area; the faults 3 and 4 appear shown in the cross section of **Fig 9**, laying towards
294 the western side at 65 and 70 degrees, as an interpretation (same as defined Fault 2 in previous
295 studies), and give the main idea that the main tectonic structure was closed to left margin of the
296 Azuela valley where the basement reached more than a 99 m depth.

297 No fault or special feature could be defined clearly on the western side of Azuela valley: only mention
298 that the inclination observed at the bottom of the valley, in cross-section, was similar to that of the
299 flanks of the valley in every margin. Thus, the eastern margin over the dam slopes inclined at 19.5°
300 and under it, 20.0° on the other hand, the western flank, on the other side of the main fault, sloped at
301 15.4°, as did the slope of its margin.

302 **7. Conclusions**

303 The application of passive seismic techniques such as the Nakamura or the H/V spectral ratio (HVSR)
304 allows large areas to be recognised without the need to distribute a longitudinal device with cables,
305 allowing the implementation of devices which are less expensive and more economical research
306 which are also faster than other ones, like boreholes. In this paper, the HVSR technique was used to

307 predict the position of the basement (bedrock) of the San Marcos dam (Ecuador) and define the cross
308 section of the Azuela River valley identifying the sediment thickness too.

309 A total of 20 points were surveyed using the HVSR technique and the relationship between the
310 frequency of natural vibration of the ground (f_o) and the thickness of the sediments (considering a
311 single layer of unconsolidated materials) was established. Following the equation type proposed by
312 Budny (1984) and developed by other authors, a power law relationship with two parameters of values
313 58.746 (scaling factor term) and -0.247 (power term) was set. When compared with data obtained
314 from performed boreholes, the new relationship proved to be capable of defining the bedrock interface
315 at San Marcos dam, achieving a coefficient of determination R^2 of 0.98 for those surveyed points
316 closer to the location of the boreholes. For the rest of the points, the results were consistent with the
317 original geological interpretation of the basin, which established a supposed depth of 95.5 to 110
318 metres in its deepest part.

319 The results obtained using the new relationship have also been compared with power relationships
320 available in the literature and which have been obtained by other authors for different materials and
321 their stratigraphic sequence. As expected, the predicted values yielded irrationality results in nearly
322 all cases, obtaining values of sediment thicknesses of more than 1000 and 2000 m, and less than 1 m
323 in shallow areas. In other cases (e.g., studies by Khan and Khan 2016), results were close to those
324 obtained with the new relationship, but only for a narrow value of f_o (i.e., between 0.9 and 3.4 Hz).

325 Having a relationship between f_o and the depth where the bedrock is expected to be found opens new
326 opportunities to enhance the knowledge of the Azuela River valley. First, an accurately cross section
327 of the Azuela valley basement could be drawn along the dam toe in order to locate and define its
328 structural features, like faults, that increased its depth. Once all the surveyed points were computed
329 and the bedrock was drawn, it could be concluded too that the inclination of the slopes of the rocky
330 substratum, at both sides of main fault, was shown to maintain the angle of the upper zone (margin
331 over the dam) with 15.4° in the western margin and in the eastern one; the slope was steeper at the

332 east side, in keeping with the geomorphology of the area. This corroborates the position of the fault
333 generated in the centre of the Azuela River valley.

334 Thus, through the application of the methodology developed in this study, geological and
335 geotechnical investigations of the position of the bedrock could be made with the application of
336 microtremors measurements in areas with direct information (boreholes as control points) as a quick
337 tool of exploration, even without a lot of boreholes. The formulations obtained could then be used in
338 all measurements of microtremor that occurred within them to obtaining coating thicknesses with an
339 accuracy of less than 4.5% (difference between depth to bedrock in boreholes and HVSR measured
340 points). This can be later extended to larger spaces with the consequent economic savings and can be
341 used in further and deeper investigations about geotechnical parameters and site response, out of the
342 scope of this work but as a new line of investigation (Ferraro et al. 2015; Kanli et al. 2006; Kanli et
343 al. 2008). Also, if the density of points suffice, tectonic structures can be defined too, like in this case.

344 **Author Contributions**

345 Conceptualization, O.Alonso and G. Torres; Data curation O.Alonso and G. Torres; Formal analysis,
346 O. Alonso; Funding acquisition, O. Alonso; Investigation, O.Alonso and G. Torres; Methodology,
347 O.Alonso; Project administration, O.Alonso; Resources, O. Alonso and F.J. Torrijo; Software,
348 O.Alonso and G. Torres; Supervision, F.J. Torrijo; Validation, F.J. Torrijo and J. Garzón- Roca;
349 Visualization, F.J. Torrijo; and J. Garzón- Roca Roles/Writing – original draft, O. Alonso and G.
350 Torres; Writing – review & editing, O. Alonso, F.J. Torrijo and J. Garzón- Roca.

351 **Funding**

352 This research received no external funding.

353 **Acknowledgements**

354 This research did not receive any specific grant from funding agencies in the public, commercial, or
355 not-for-profit sectors. Special thanks to Dirección del Canal de Riego Cayambe-Pedro Moncayo
356 (GAD de la Provincia de Pichincha), and its Director, Mr. Rene Espín, to let to use the base

357 information and access to place. The authors fully acknowledge the financial support provided by the
358 Department of Geological and Geotechnical Engineering of the UPV. Also, thanks to GEOTOP
2
359 Ecuatorial Consulting (geotecnia2015@gmail.com) for the support provided and the equipment used
4
5
360 in the research.
7
8

361 **Conflicts of Interest**

10
11
362 The authors declare no conflict of interest.
13
14

363 **References**

16
17
364 Albarello D, Cakir R, Walsh TJ (2011) Single station ambient vibration measurements in the Puget
19
20
365 lowland and coastal area, Washington. DNR-DGER internal report.
21
22
23

24
366 Alvarado A (2012) Néotectonique et cinématique de la déformation continentale en Equateur. Thèse
25
26
367 pour obtenir le grade de Docteur de L'Université de Grenoble, Spécialité: Sciences de la Terre,
27
28
368 l'Univers, et l'Environnement. France.
30
31

32
369 Asten MW (2004) Comment on "Microtremor observations of deep sediment resonance in
33
34
370 metropolitan Memphis, Tennessee" by Paul Bodin, Kevin Smith, Steve Horton and Howard Hwang.
35
36
371 Engineering Geology <https://doi.org/10.1016/j.enggeo.2003.09.001>
38
39

40
372 Bard PY and SESAME participants (2004) The SESAME Project: An overview and main results.
41
42
373 13th World Conference on Earthquake Engineering. Paper No. 2207. Vancouver, Canada
43
44
45

46
374 Birgören G, Özel O, Syahi B (2009) Bedrock Depth Mapping of the Coast South of İstanbul:
47
48
375 Comparison of Analytical and Experimental Analyses. Turkish Journal of Earth Sciences
49
50
376 <http://doi.org/10.3906 / place-0712-3>
52
53

54
377 Bonnefoy-Claudet S, Cornou C, Bard PY, Cotton F, Moczo P, Kristek J, Fäh D 2006 H/V ratio: a
55
56
378 tool for site effects evaluation. Results from 1-D noise simulations. Geophysical Journal Int.
57
58
379 <http://doi.org/10.1111/j.1365-246X.2006.03154.x>
60
61
62
63
64
65

- 380 Budny M (1984) SeismischeBestimmung der BodendynamischenKennwerte von
381 oberflächennahenSchichten in Erdbebengebieten der niederheinischenBucht und
2
3
382 ihreingenieurseismologischeAnwendung. PhD Thesis, Geol. Inst. University of Cologne Spec. Publ.
4
5
383 57, 208 pp
7
8
384 Chang Y-W, Van Bang P, Loh Ch-H (2015) Identification of Basin Topography Characteristic Using
10
11
385 Multivariate Singular Spectrum Analysis: Case Study of the Taipei Basin. Engineering Geology
12
13
386 <https://doi.org/10.1016/j.enggeo.2015.08.027>
15
16
17
387 Delgado J, Garrido J, Lenti L, Lopez-Casado C, Martino S, Sierra FJ (2015) Unconventional
18
19
388 pseudostatic stability analysis of the Diezma landslide (Granada, Spain) based on a high-resolution
21
22
389 engineering-geological model. Engineering Geology
23
24
390 <http://dx.doi.org/10.1016/j.enggeo.2014.11.002>
25
26
27
391 Egüez A, Aspden J (1993) The Meso-Cenozoic evolution of the Ecuadorian Andes. Memory of
29
30
392 Second International Symposium Andean Geodynamics. Ext. Abstract 78-181 Oxford, UK
31
32
33
393 Ferraro A, Grasso S, Massimino MR, Maugeri M (2015) Influence of geotechnical parameters and
35
36
394 numerical modelling on local seismic response analysis. Proceedings of the XVI ECSMGE,
37
38
395 Geotechnical Engineering for Infrastructure and Development <http://doi.org/10.1680/ecsmge.60678>
39
40
41
396 Field EH, Jacob KH (1995) A comparison and test of various site response estimation techniques,
43
44
397 including three that are not reference site dependent. Bulletin of the Seismological Society of America
45
46
398 85(4):1127-1143
48
49
50
399 G.A.D. de la Provincia de Pichincha (GADPP) (2009). Estudios de geología y geotecnia dentro del
51
52
400 Proyecto de Riego Cayambe Tabacundo y agua potable Pesillo-Imbabura, cantón Cayambe, provincia
53
54
401 de Pichincha. Informe Definitivo. Quito
56
57
58
59
60
61
62
63
64
65

- 402 García-Jerez A, Luzón F, Navarro M, Pérez-Ruíz JA (2006) Characterization of the sedimentary
403 cover of the Zafarraya basin (Southern Spain) by means of ambient noise. Bulletin of the
2
3
404 Seismological Society of America <http://doi.org/10.1785/0120050061>
4
5
6
405 Hellel M, Oubaiche EH, Chatelain J et al. (2019) Efficiency of ambient vibration HVS
8
406 investigations in soil engineering studies: backfill study in the Algiers (Algeria) harbor container
10
11
407 terminal. Bull. Eng. Geol. Environ <https://doi.org/10.1007/s10064-018-01458-y>
12
13
14
408 Hinzen KG, Scherbaum F, Weber B (2004) On the resolution of H/V measurements to determine
16
17
409 sediment thickness, a case study across a normal fault in the Lower Rhine Embayment, Germany.
18
19
410 Journal of Earthquake Engineering <http://doi.org/10.1080/13632460409350514>
21
22
411 Ibs Von Seht M, Wohlenberg J (1999) Microtremor measurements used to map thickness of soft
24
25
412 sediments. Bulletin of Seismological Society of America <https://doi.org/10.1785/BSSA0890010250>
26
27
28
413 Jirasakjamroonsri A, Poovarodom N, Warnitchai P (2019) Seismic site characteristics of shallow
30
31
414 sediments in the Bangkok Metropolitan Region, and their inherent relations. Bull. Eng. Geol. Environ.
32
33
415 <https://doi.org/10.1007/s10064-017-1220-3>
34
35
36
416 Kanli AI (2010) Integrated approach for surface wave analysis from near-surface to bedrock. In:
38
39
417 Miller RD, Bradford JD, Holliger K (eds) Advances in Near-Surface Seismology and Ground-
40
41
418 Penetrating Radar, Geophysical Developments Series No. 15:461-476. SEG Reference Publications,
43
44
419 Tulsa, Oklahoma (USA).
45
46
47
420 Kanli AI, Kang T-S, Pınar A, Tildy P, Prónay Z (2008) A Systematic geophysical approach for site
48
49
50
51
52
53
421 response of the Dinar Region, South Western Turkey. Journal of Earthquake Engineering
54
55
422 <https://doi.org/10.1080/13632460802013966>
56
57
58
423 Kanli AI, Tildy P, Prónay Z, Pınar A, Hermann L (2006) V_{s30} Mapping and soil classification for
59
60
424 seismic site effect evaluation in Dinar Region, SW Turkey. Geophysical Journal International
61
62
425 <https://doi.org/10.1111/j.1365-246X.2006.02882.x>
63
64
65

- 426 Khan S, Khan MA (2016) Mapping sediment thickness of Islamabad city using empirical
427 relationships: Implications for seismic hazard assessment. *J Earth Syst Sci*
2
3
428 <https://doi.org/10.1007/s12040-016-0675-0>
4
5
6
429 Konno K, Ohmachi T (1998) Ground-Motion Characteristics Estimated from Spectral Ratio between
8
430 Horizontal and Vertical Components of Microtremor. *Bulletin of Seismological Society of America*
10
11
431 88(1):228-241.
12
13
14
432 Lermo JF, Lermo S, Chavez-Garcia J (1992) Site Effect Evaluation using microtremors: a review
16
17
433 (abstract). *EOS* 73, 352.
18
19
20
434 Nakamura Y (1989) A method for dynamic characteristics estimation of subsurface using
22
435 microtremors on the ground surface. *Quarterly Report of Railway Technical Research Institute*
24
25
436 (RTRI) 30:25-33
26
27
28
437 Ohmachi T, Nakamura Y, Toshinawa T (1991) Ground Motion Characteristics in the San Francisco
30
438 Bay Area detected by Microtremor Measurements. *International Conferences on Recent Advances in*
32
33
439 *Geotechnical Earthquake Engineering and Soil Dynamics*, 11-15 March, 1643-1648 St. Louis,
35
440 Missouri Paper LP08
37
38
39
441 Pamuk E, Özdağ ÖC, Akgün M (2019) Soil characterization of Bornova Plain (Izmir, Turkey) and
41
442 its surroundings using a combined survey of MASW and ReMi methods and Nakamura's (HVSr)
43
443 technique. *Bull. Eng. Geol. Environ.* <https://doi.org/10.1007/s10064-018-1293-7>
45
46
47
444 Parolai S, Bormann P, Milkereit C (2002) New relationships between Vs, thickness of sediments, and
49
50
51
445 resonance frequency calculated by the H/V ratio of seismic noise for Cologne Area (Germany).
52
446 *Bulletin of Seismological Society of America* <https://doi.org/10.1785/0120010248>
53
54
55
447 Samaniego P, Monzier M, Robin C, Hall ML (1998) Late Holocene eruptive activity at Nevado
57
448 Cayambe Volcano, Ecuador. *Bulletin of Volcanology* 59:451-459
58
59
60
61
62
63
64
65

- 449 Samaniego P, Eissen J-P, Monzier M, Robin C, Alvarado A, Yepes H (2004) Los peligros volcánicos
450 asociados con el Cayambe. Instituto Geofísico, Quito
2
3
4
451 SESAME (2004) Guidelines for the implementation of the H/V spectral ratio technique on ambient
5
6
452 vibrations: SESAME, European project, WP12. Deliverable D23.12.
8
9
10
453 Torres GF (2018) La amenaza sísmica y volcánica de la presa de la laguna San Marcos. Cayambe-
11
12
454 Pichincha. Trabajo de Titulación (BsC Thesis). Universidad Central de Ecuador. Quito
13
14
455 <http://www.dspace.uce.edu.ec/handle/25000/16316>. Accessed 19 may 2019
16
17
18
456 Vella A, Galea P, D'Amico S (2013) Site frequency response characterization of the Maltese islands
19
20
457 based on ambient noise H/V ratios. Engineering Geology
21
22
458 <https://doi.org/10.1016/j.enggeo.2013.06.006>
24
25
26
27
28
29
30
31
32
33
34
35
36
37
38
39
40
41
42
43
44
45
46
47
48
49
50
51
52
53
54
55
56
57
58
59
60
61
62
63
64
65

459 **List of Figures**

460 **Fig. 1** Location of San Marcos dam area (adapted from Torres 2008).

461 **Fig. 2** San Marcos dam area geological map (adapted from Torres 2018).

462 **Fig. 3** San Marcos dam longitudinal profile. Geological interpretation in preliminary studies for its
463 construction with the position of the HVSR surveys (blue triangles) and the used contrast boreholes
464 (bold red lines). A simplified representation of the materials defined in the geotechnical studies of the
465 dam is included: fine alluvial and lacustrine sediments (1), coarse and gravel sediments of alluvial
466 origin (2), coarse sediments and intercalations of volcanic materials (3), Cayambe pyroclastic flows
467 (4), basaltic basement composed by volcanic lava of the Angochagua Formation (5), and colluvial
468 sediments (6). Orientation east-west at scale 1H:2V. Adapted from original with permission of
469 GADPP (2009).

470 **Fig. 4** Surveyed points location around San Marcos dam, in the Azuela valley. Points 18,19, and 20
471 were performed over the dam. Points 1, 4, 7, 10, 12, 14, and 17 were considered as a projection in
472 delineated cross section of valley (dashed purple line).

473 **Fig. 5** (A) Raw data example from Point 1. In order, N-S, E-W and Z components. (B) Windowing
474 example from raw data applied at Point 2 record with 48 windows selected (20 s). Anti-triggering
475 filters were applied to raw data and filtered data. Components N-S, E-W and Z in order from up to
476 down. (C) Equipment used in this investigation at point 19

477 **Fig. 6** Final results from H/V analysis on selected surveyed points from total performed. Grey bands
478 show the fundamental frequency of vibration and its standard deviation.

479 **Fig. 7** Adjusted curve $Z=af_0^b$ for data given in **Table 3**.

480 **Fig. 8** f_0 versus sediment thickness curves in the different investigations related in **Table 2**.

481 **Fig. 9** Geological cross section of Azuela valley obtained after the application of passive techniques
482 of the seismic method (HVSR). Basement (lavas from Angochagua Formation) position obtained in
483 this study is delineated in bold dashed black line. It can be compared with old construction
484 interpretation section of basement represented in solid color. Vertical blue line represent depth at

485 every surveyed point and dot and dash blue lines are projected HVSR surveys over the section.

486 Boreholes used are drawn in red line (depth to basement). Scale 1H:2V

2
3
4
5
6
7
8
9
10
11
12
13
14
15
16
17
18
19
20
21
22
23
24
25
26
27
28
29
30
31
32
33
34
35
36
37
38
39
40
41
42
43
44
45
46
47
48
49
50
51
52
53
54
55
56
57
58
59
60
61
62
63
64
65

487 **List of Tables**

488 **Table 1** Results obtained in present investigation with fundamental frequency (f_o), amplification (A_o)
2
3
489 and period (T_o) of the 20 measured points
4

490 **Table 2** Value of a and b coefficients to the equation defined by Budny (1984) given by different
7
491 authors, also including the present investigation. R^2 obtained and materials where were performed are
9
10 also indicated
11
12

1493 **Table 3** Referred boreholes with depth data of basement (in metres) and HVSR surveys performed
14
15 as control correlation with fundamental frequency (f_o)
16

1495 **Table 4** Depth of basement (bedrock) predicted by different authors equations (in metres) compared
19
20 to the present investigation (third column) based on fundamental frequency f_o
21
22
23
24
25
26
27
28
29
30
31
32
33
34
35
36
37
38
39
40
41
42
43
44
45
46
47
48
49
50
51
52
53
54
55
56
57
58
59
60
61
62
63
64
65

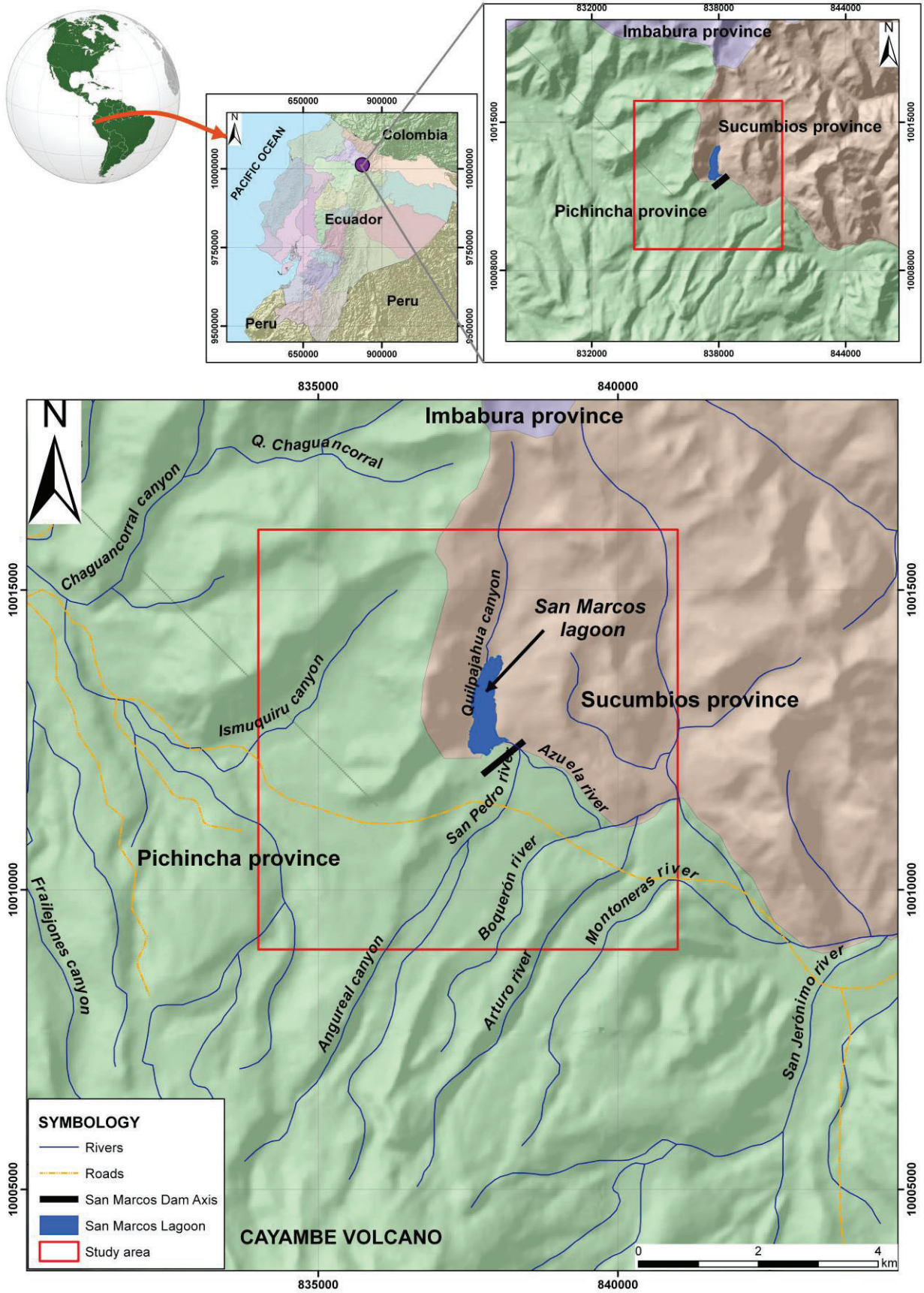


Fig. 1. Location of San Marcos dam area (adapted from Torres 2008)

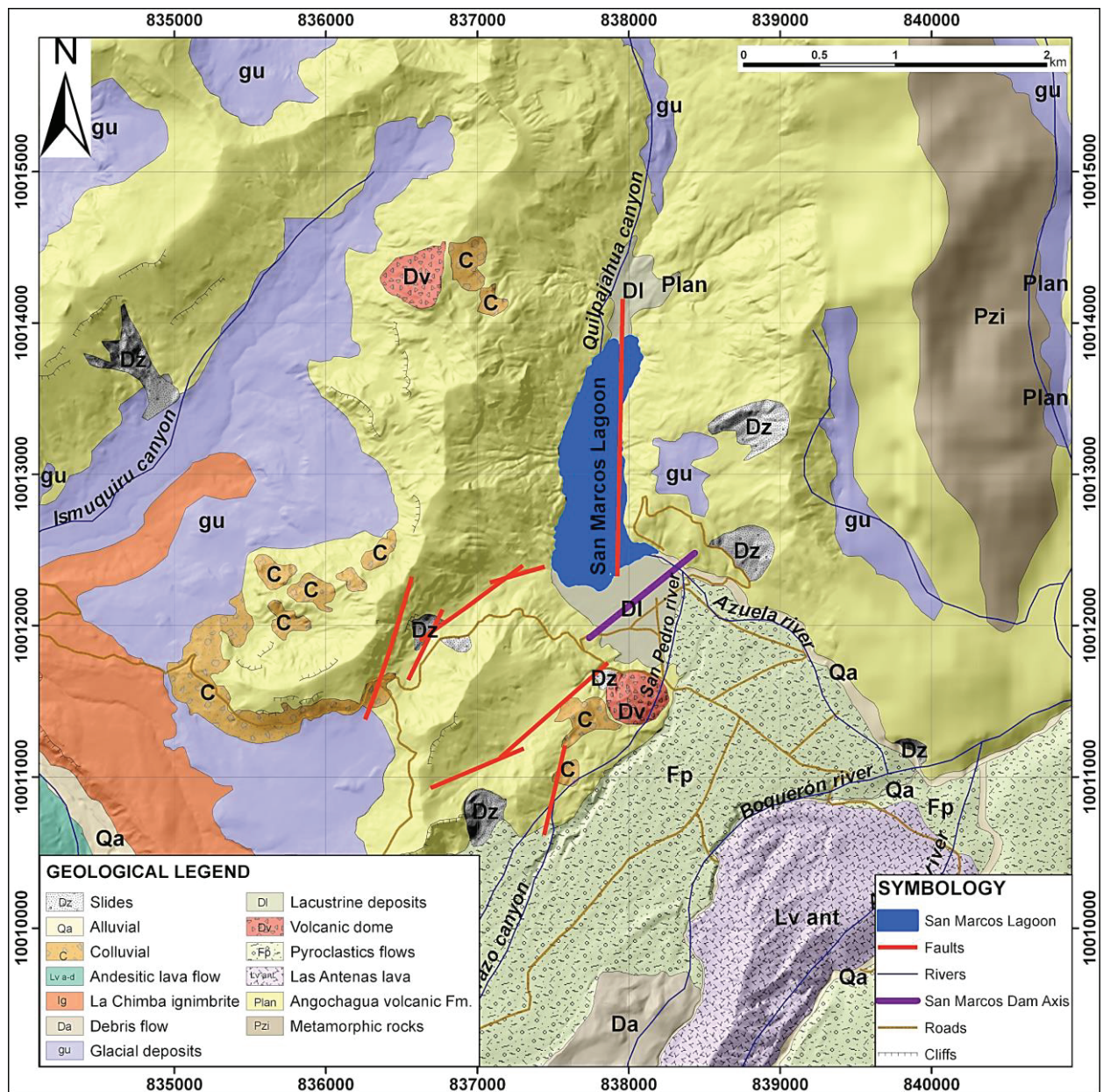


Fig. 2. San Marcos dam area geological map (adapted from Torres 2018).

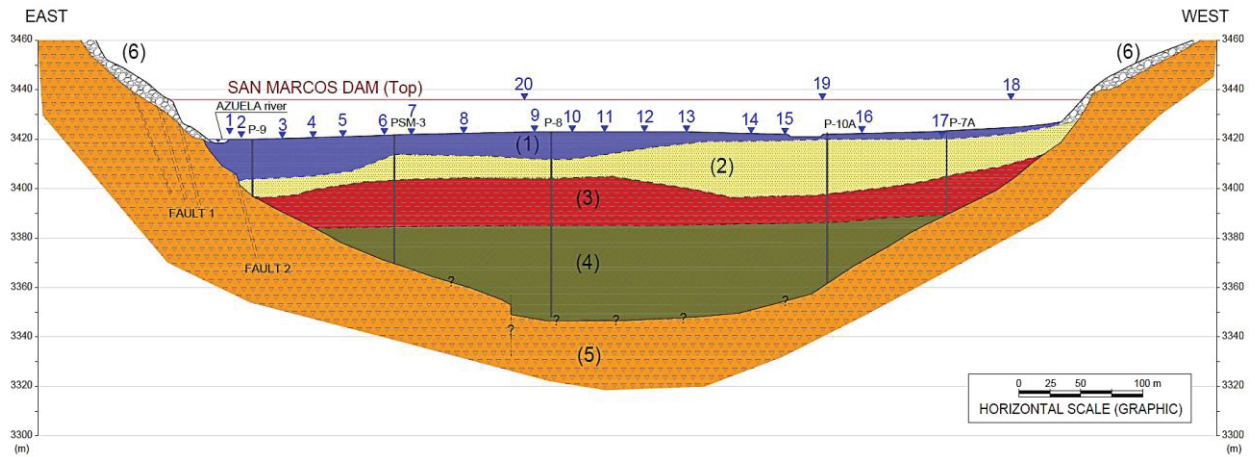


Fig. 3. San Marcos dam longitudinal profile. Geological interpretation in preliminary studies for its construction with the position of the HVSR surveys (blue triangles) and the used contrast boreholes (bold red lines). A simplified representation of the materials defined in the geotechnical studies of the dam is included: fine alluvial and lacustrine sediments (1), coarse and gravel sediments of alluvial origin (2), coarse sediments and intercalations of volcanic materials (3), Cayambe pyroclastic flows (4), basaltic basement composed volcanic lava of the Angochagua Formation (5), and colluvial sediments (6). Orientation east-west at scale 1H:2V. Adapted from original with permission of GADPP (2009)

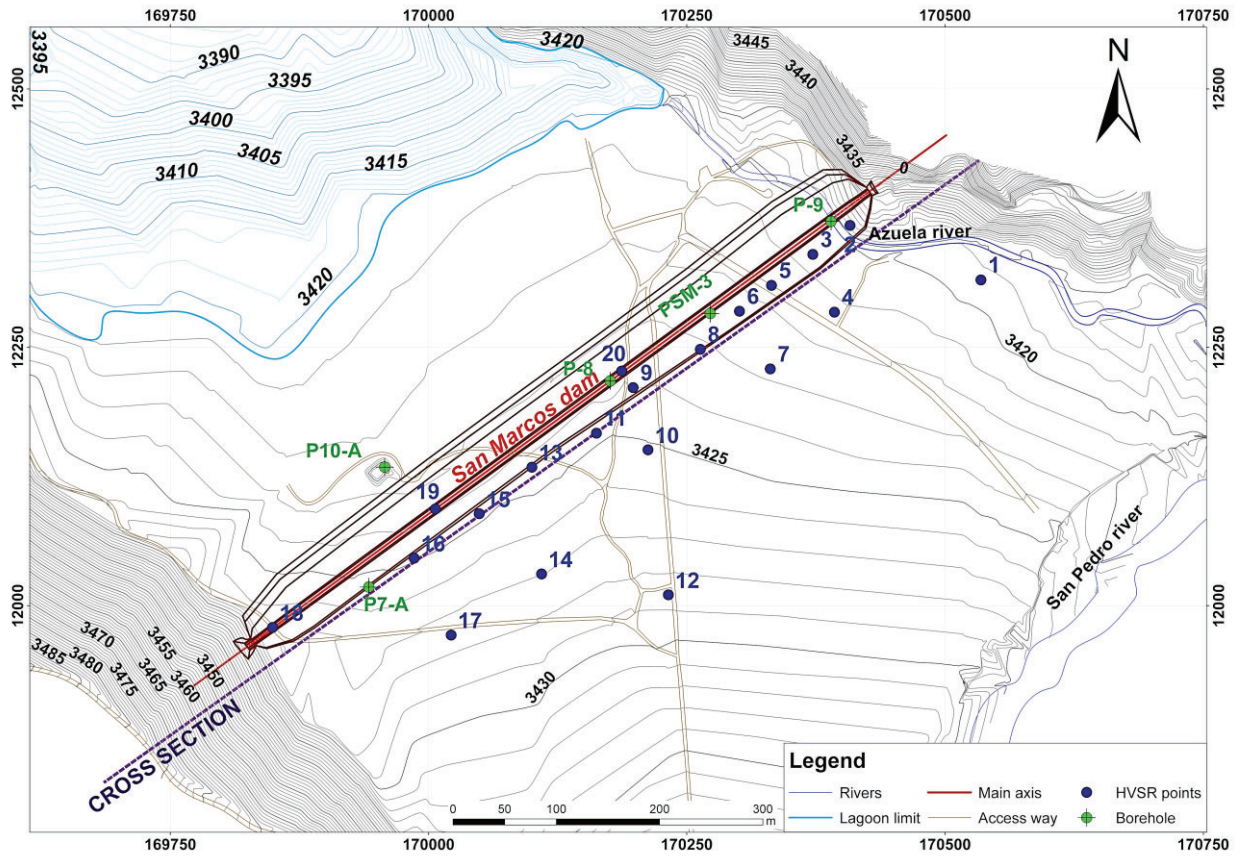


Fig. 4. Surveyed points location around San Marcos dam, in the Azuela valley. Points 18,19, and 20 were performed over the dam. Points 1, 4, 7, 10, 12, 14, and 17 were considered as a projection in delineated cross section of valley (dashed purple line).

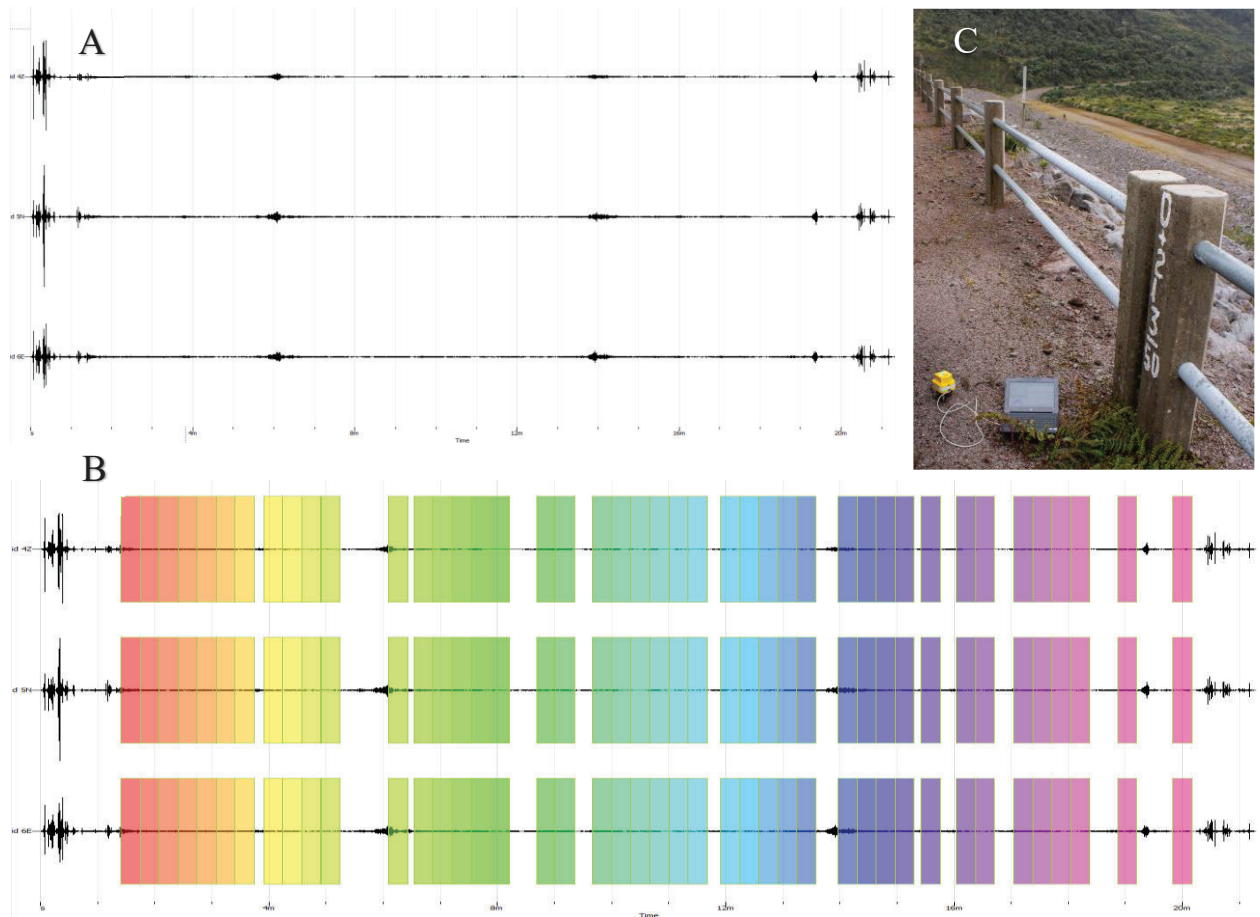


Fig. 5. (A) Raw data example from Point 1. In order, N-S, E-W and Z components. (B) Windowing example from raw data applied at Point 2 record with 48 windows selected (20 s). Anti-triggering filters were applied to raw data and filtered data. Components N-S, E-W and Z in order from up to down. (C) Equipment used in this investigation at point 19

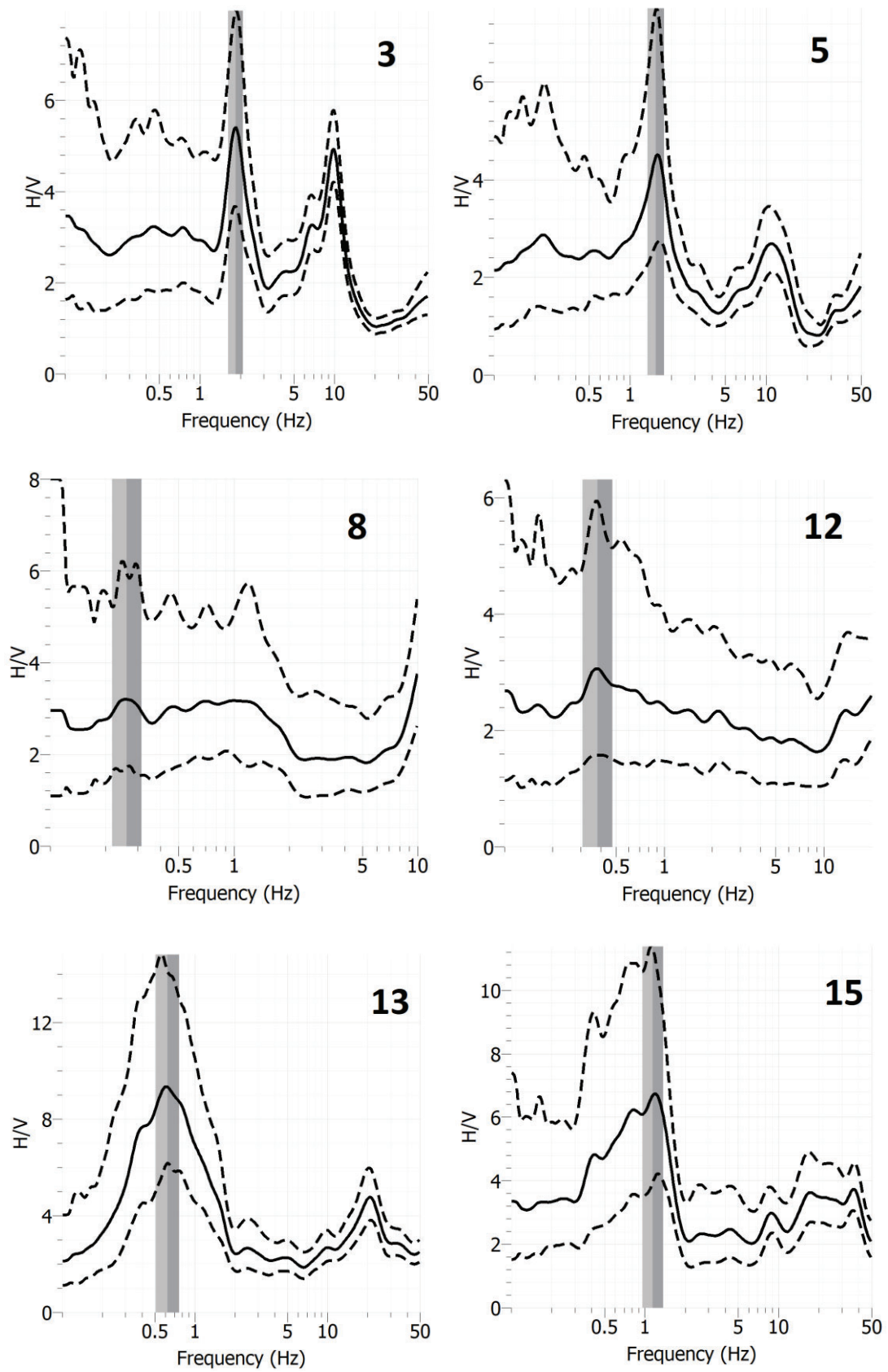


Fig. 6. Final results from H/V analysis on selected surveyed points from total performed. Grey bands show the fundamental frequency of vibration and its standard deviation

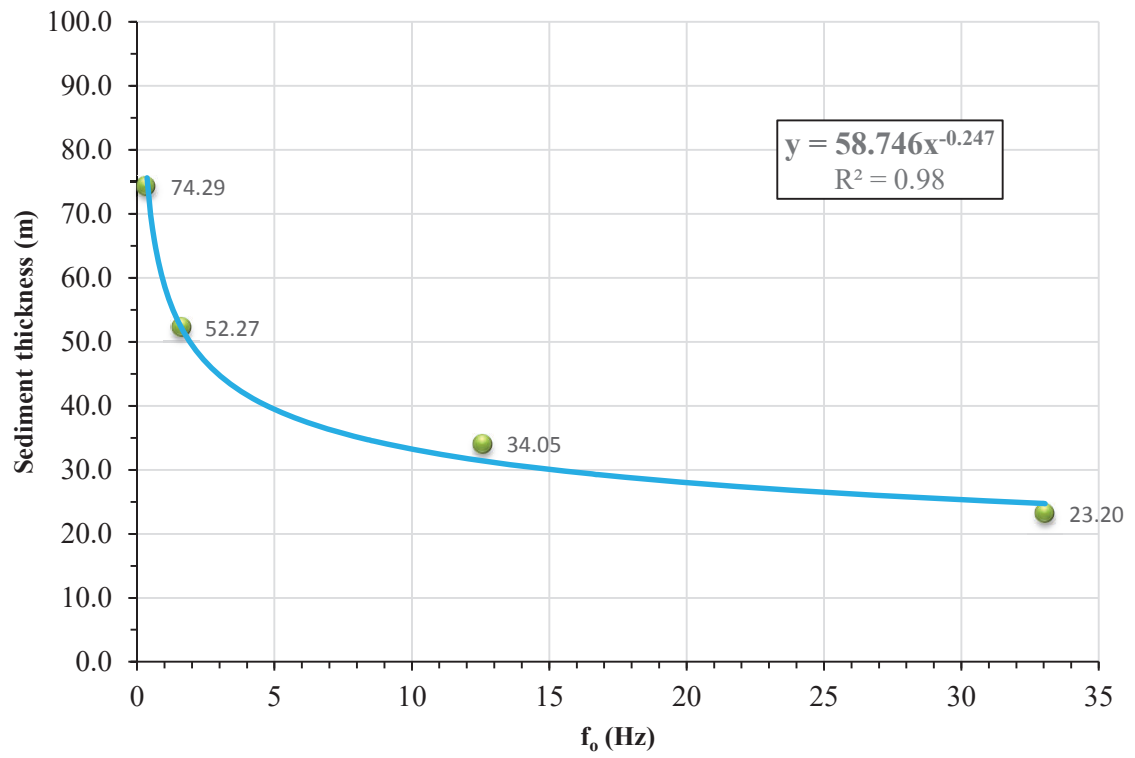


Fig. 7. Adjusted curve $Z = a f_0^b$ for data given in **Table 3**.

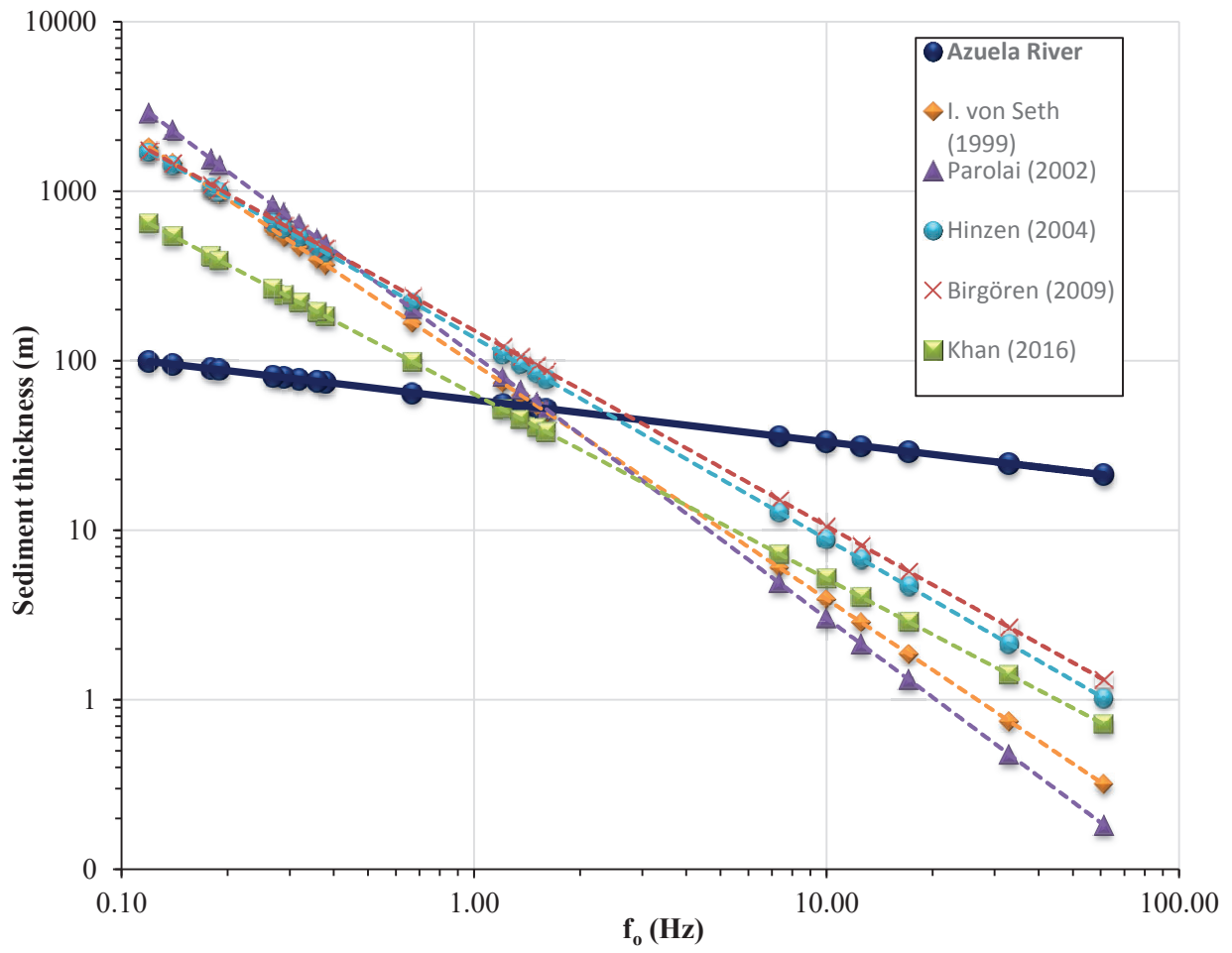


Fig. 8. f_0 versus sediment thickness curves in the different investigations related in **Table 2**.

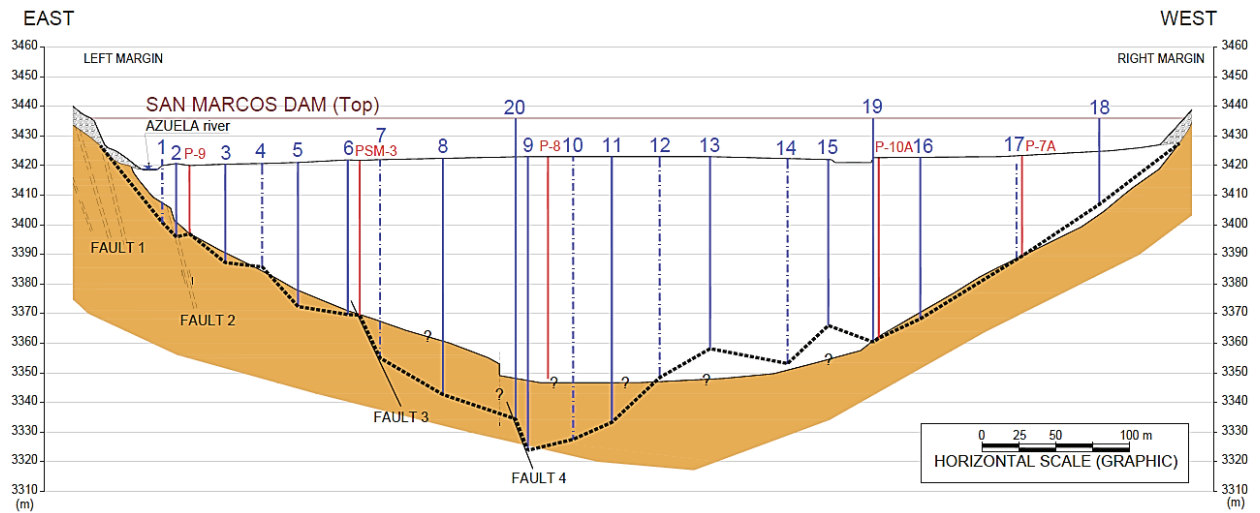


Fig. 9. Geological cross section of Azuela valley obtained after the application of passive techniques of the seismic method (HVSr). Basement (lavas from Angochagua Formation) position obtained in this study is delineated in bold dashed black line. It can be compared with old construction interpretation section of basement represented in solid color. Vertical blue line represent depth at every surveyed point and dot and dash blue lines are projected HVSr surveys over the section. Boreholes used are drawn in red line (depth to basement). Scale 1H:2V

Table 1. Results obtained in present investigation with fundamental frequency (f_o), amplification (A_o) and period (T_o) of the 20 measured points.

POINT	f_o (Hz)	A_o	T_o (s)
1	<i>61.26</i>	1.90	0.02
2	<i>33.05</i>	3.45	0.03
3	<i>10.01</i>	4.94	0.10
4	<i>7.36</i>	1.58	0.14
5	<i>1.51</i>	4.92	0.66
6	<i>1.61</i>	3.70	0.62
7	<i>0.32</i>	1.65	3.13
8	<i>0.29</i>	3.36	3.45
9	<i>0.12</i>	3.10	8.33
10	<i>0.14</i>	3.31	7.14
11	<i>0.18</i>	2.14	5.56
12	<i>0.38</i>	2.81	2.63
13	<i>0.67</i>	8.74	1.49
14	<i>0.27</i>	9.33	3.70
15	<i>1.21</i>	5.35	0.83
16	<i>1.36</i>	5.17	0.74
17	<i>12.58</i>	4.49	0.08
18	<i>17.11</i>	7.42	0.06
19	<i>0.36</i>	2.37	2.78
20	<i>0.19</i>	3.61	5.26

Table 2. Value of a and b coefficients to the equation defined by Bundy (1984) given by different authors, also including the present investigation. R^2 obtained and materials where were performed are also indicated.

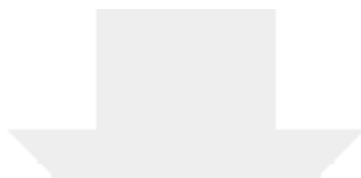
INVESTIGATION	a	b	R^2	MATERIALS
Ibs von Seth and Wohlenberg (1999)	96.000	-1.388	0.981	Sedimentary covers of Tertiary and Quaternary ages (Rhin River)
Parolai <i>et al.</i> (2002)	108.000	-1.551		Gravel, sand, and clays mainly
Hinzen <i>et al.</i> (2004)	137.000	-1.190		Well-sorted marine sand and consolidated clay (Rhin River)
Birgören <i>et al.</i> (2009)	150.990	-1.153	0.995	Dense sand, silty sand, clayey sand, gravel and clay
Khan and Khan (2016)	63.680	-1.090	0.990	Interbedded sandy silt and limestone gravel, aeolian loess
PRESENT STUDY	58.746	-0.247	0.98	Alluvial and lacustrine sediments, volcanoclastic sediments and pyroclastic flows

Table 3. Referred boreholes with depth data of basement (in metres) and HVSR surveys performed as control correlation with fundamental frequency (f_0)

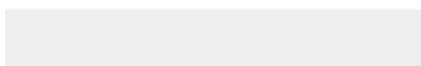
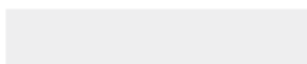
BOREHOLE	BASEMENT	POINT	f_0
P - 9	23.20	2	33.05
PSM - 3	52.27	6	1.61
P - 7 A	34.05	17	12.58
P – 10 A	74.29	19	0.36

Table 4. Depth of basement (bedrock) predicted by different authors equations (in metres) compared to the present investigation (third column) based on fundamental frequency f_0

HVSR POINT	f_0 (Hz)	THIS STUDY (m)	Ibs von Seth (1999)	Parolai (2002)	Hinzen (2004)	Birgören (2009)	Khan (2016)
1	<i>61.26</i>	21.3	0.3	0.2	1.0	1.3	0.7
2	<i>33.05</i>	24.8	0.7	0.5	2.1	2.7	1.4
3	<i>10.01</i>	33.3	3.9	3.0	8.8	10.6	5.2
4	<i>7.36</i>	35.9	6.0	4.9	12.7	15.1	7.2
5	<i>1.51</i>	53.1	54.2	57.0	83.9	93.9	40.6
6	<i>1.61</i>	52.2	49.6	51.6	77.7	87.2	37.9
7	<i>0.32</i>	77.8	466.8	632.3	531.6	561.8	220.5
8	<i>0.29</i>	79.8	535.1	736.6	597.7	629.3	245.5
9	<i>0.12</i>	99.2	1821.2	2894.8	1708.0	1740.8	642.2
10	<i>0.14</i>	95.5	1470.4	2279.2	1421.8	1457.3	542.9
11	<i>0.18</i>	89.7	1037.4	1543.5	1054.3	1090.7	412.8
12	<i>0.38</i>	74.6	367.7	484.4	433.3	460.8	182.8
13	<i>0.67</i>	64.9	167.4	201.0	220.6	239.6	98.5
14	<i>0.27</i>	81.2	590.9	823.0	650.7	683.3	265.3
15	<i>1.21</i>	56.0	73.7	80.4	109.2	121.2	51.7
16	<i>1.36</i>	54.4	62.6	67.0	95.0	105.9	45.5
17	<i>12.58</i>	31.4	2.9	2.1	6.7	8.1	4.0
18	<i>17.11</i>	29.1	1.9	1.3	4.7	5.7	2.9
19	<i>0.36</i>	75.6	396.4	526.7	462.1	490.4	193.9
20	<i>0.19</i>	88.5	962.4	1419.3	988.6	1024.7	389.2




Click here to access/download
Supplementary Material
Certificate_202105-25165823.pdf



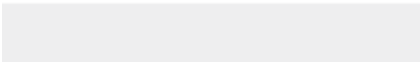
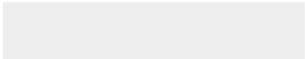



Click here to access/download
Supplementary Material
Cover letter Review.docx



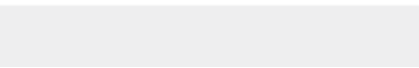
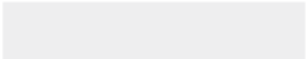


Click here to access/download
Supplementary Material
Cover letter Editors.docx





Click here to access/download
Supplementary Material
Title Page.docx





Click here to access/download
Supplementary Material
Highlights.docx

